

## ON THE WAY OF GROWING $\text{YBa}_2\text{Cu}_3\text{O}_{7-x}$ SUPERCONDUCTING THIN FILMS FROM A FLUORIN-FREE WATER BASED PROPIONATE PRECURSOR SOLUTION

CORNELIA BOGĂȚAN (POP)<sup>a</sup>, MIRCEA NĂSUI<sup>a</sup>, TRAIAN PETRIȘOR JR.<sup>a</sup>,  
MIHAI GABOR<sup>a</sup>, TANIA RISTOIU<sup>a</sup>, LELIA CIONTEA<sup>a</sup>,  
TRAIAN PETRIȘOR<sup>a</sup>

**ABSTRACT.**  $\text{YBa}_2\text{Cu}_3\text{O}_{7-x}$  thin films were successfully deposited from a water-based propionate precursor solution. In order to determine the thermal decomposition behaviour of the deposited precursor solution during the pyrolysis, the precursor powder, as- obtained by drying the precursor solution, was submitted to thermal analysis (DTA – TG). The precursor films were deposited on (100)  $\text{SrTiO}_3$  single crystalline substrates by spin-coating and subjected to a single – step thermal treatment comprising both pyrolysis and crystallization. The as-obtained  $\text{YBa}_2\text{Cu}_3\text{O}_{7-x}$  films were structurally and morphologically investigated by X-ray diffraction and atomic force microscopy, respectively. The electrical characterization of the films was made by the four point method.

**Keywords:** *YBCO thin films, superconductivity, spin coating deposition, thermal analysis, film characterization*

### INTRODUCTION

$\text{YBa}_2\text{Cu}_3\text{O}_{7-x}$  (YBCO) films have gained considerable interest due to their intrinsic properties. Because of these properties the YBCO superconducting films are very promising for power applications. These films can be obtained by both physical, and chemical methods [1,2]. The chemical solution deposition (CSD) is a low cost, high rate and a non-vacuum method which complies with the industrial demands [3].

The most common CSD method used in order to obtain superconducting YBCO films is the metal-organic decomposition of trifluoroacetates (TFA-MOD) [4]. By this method epitaxial YBCO films with very good superconducting properties ( $J_c \approx 10 \text{ MA/cm}^2$ ) were obtained [5]. However, this method has a major drawback: during the thermal decomposition of the precursor solution, highly toxic and corrosive acid is released, namely the hydrofluoric acid (HF).

---

<sup>a</sup> Technical University of Cluj-Napoca, Materials and Enviromental Faculty, 28 Memorandumului Street, RO-400114, Cluj-Napoca, Romania, corneliapop@yahoo.com

To overcome this disadvantage, several research groups have begun to investigate fluorine-free precursor solutions using different combinations of starting reagents and solvents.

Thus, several groups have succeeded to obtain superconducting YBCO films with good superconducting properties using the corresponding metal acetylacetonates and both pyridine, and propionic acid as solvents [6]. In order to obtain epitaxial YBCO films they have used a low-cost vacuum technique during the thermal treatment.

Another research group have used Y, Ba, Cu trimethylacetates and a combination of propionic acid and amines as solvents [7]. Good results have also been reported when using metal acetates dissolved in a mixture of water and acetic acid [8].

The aim of this work was to find a new, simpler and more ecologic precursor solution (in our case a water based precursor solution) from which YBCO superconducting films can be obtained.

## RESULTS AND DISCUSSION

### Precursor Powder Characterization

The precursor powder has been obtained by drying the final precursor solution in air at 60°C on a hot plate (the preparation of the final precursor solution is detailed in the **Experimental section**).

The thermal decomposition behavior of the precursor powder gives us important clues regarding the thermal treatment used for obtaining YBCO films. In order to find out the optimal conditions for the thermal treatment, the precursor powder was subjected to thermal analyses. The analyses were performed in dry and humid oxygen, from room temperature up to 500°C, at different heating rates. These different heating rates are needed for the highly exothermic reactions that take place during the decomposition of the propionate complex. The DTA – TG curves of the precursor powder are presented in figure 1.

As it can be seen, the thermal decomposition of the precursor solution ends around 400°C both in dry, and humid oxygen atmosphere. According to figure 1 the thermal decomposition of the precursor powder takes place as follows:

- In the first stage, in the temperature range 20°C – 200°C, the precursor powder goes through a dehydration process indicated on the DTA curves by an endothermic peak at 197°C. In this stage the thermogravimetric curves show a weight loss of 4%, both in humid and in dry oxygen atmosphere.

- In the temperature range  $200^\circ\text{C} - 260^\circ\text{C}$ , the second stage of the thermal decomposition performed in dry oxygen, begins the decomposition of the organic part of the precursor powder. This is indicated by a weight loss of 23% on the TG curve and by two exothermic peaks on the DTA curve at  $238^\circ\text{C}$  and  $252^\circ\text{C}$ , respectively.
- The third stage of the decomposition process for the precursor powder treated in dry oxygen atmosphere is in the temperature range  $260^\circ\text{C} - 300^\circ\text{C}$ . In this stage it can be easily observed that the TG curve registers a slight weight increase that reveals the oxidation of Cu(I) to Cu(II) [9].
- For the precursor powder thermally treated in humid oxygen atmosphere the second stage of the decomposition process takes place in the temperature range  $200^\circ\text{C} - 300^\circ\text{C}$ . During this stage the beginning of the organic part decomposition is indicated by a weight loss of 25 % on the TG curve and by the presence of two exothermic peaks on the DTA curve at  $235^\circ\text{C}$  and  $270^\circ\text{C}$ .
- The last stage of the thermal decomposition of the precursor powder thermally treated both in dry and humid oxygen atmosphere is in the temperature range  $300^\circ\text{C} - 400^\circ\text{C}$ . The DTA curve registered in dry oxygen atmosphere presents three exothermic peaks at  $366^\circ\text{C}$ ,  $384^\circ\text{C}$  and at  $398^\circ\text{C}$  showing the finalization of the organic part decomposition. The corresponding thermogravimetric curve reveals a weight loss of 19%. In humid oxygen the DTA curve presents only two exothermic peaks: a small peak at  $321^\circ\text{C}$  and a very sharp peak at  $398^\circ\text{C}$ , indicating that the decomposition reactions are partially overlapped. The corresponding TG curve registers a weight loss of 21%.

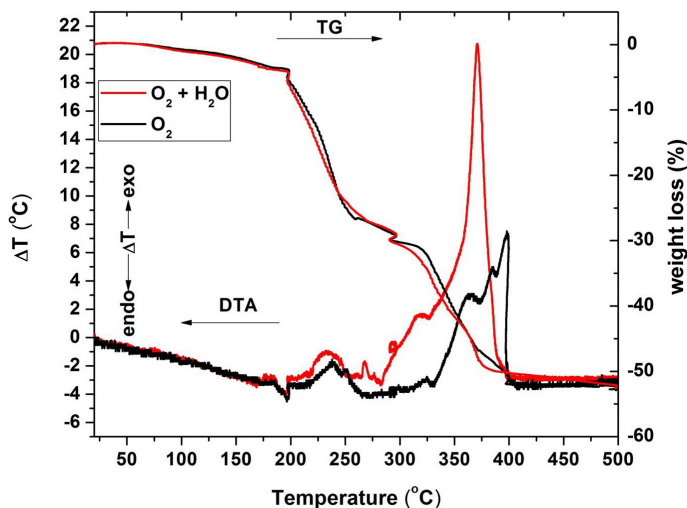


**Figure 1.** DTA – TG analyses performed under dry and humid oxygen atmosphere

Above of 400°C the TG – DTA curves are stable, indicating that the thermal decomposition of the sample is complete.

In order to identify the crystalline phases that are present in the powder sample during the thermal decomposition process the precursor powders thermally treated at different temperatures (300°C, 400°C and 500°C) were subjected to X-ray diffraction. The X-ray patterns are presented in figure 2.

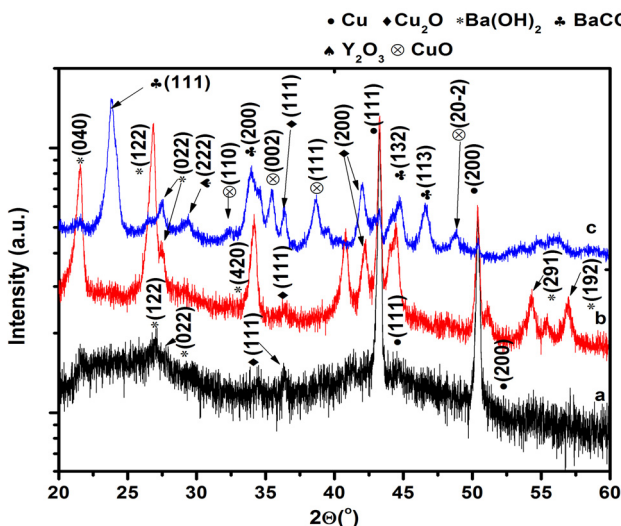


**Figure 2.** X-ray diffraction patterns of the precursor powders thermally treated at: (a) 300°C, (b) 400°C and (c) 500°C

As it can be observed at the temperature of 300°C in the precursor powder are present the following crystalline phases: metallic Cu – (111)Cu and (200)Cu, Cu<sub>2</sub>O – (111)Cu<sub>2</sub>O, and Ba(OH)<sub>2</sub> – (122)Ba(OH)<sub>2</sub> and (022)Ba(OH)<sub>2</sub>. As it can be seen at 400°C the intensity of the peaks corresponding to metallic Cu phase decreases, while the intensity and the numbers of the peaks corresponding to Cu<sub>2</sub>O phase are increasing. This indicates the oxidation of a large amount of metallic Cu to Cu<sub>2</sub>O. It can also be observed that the peaks corresponding to Ba(OH)<sub>2</sub> are more intens, indicating a more advance crystalization of barium hidroxide. At 500°C along with the Cu<sub>2</sub>O phase, the CuO phase is present proving the Cu(I) to Cu(II) oxidation supposition. Also at 500°C the X-ray diffraction pattern exhibits peaks corresponding to Y<sub>2</sub>O<sub>3</sub> phase. At this temperature Ba(OH)<sub>2</sub> reacts with the atmospheric CO<sub>2</sub> and peaks corresponding to BaCO<sub>3</sub> can be observed in the X-ray diffraction patterns.

The crystalline phases present in the precursor powder (and also in the film) after the pyrolysis are: Y<sub>2</sub>O<sub>3</sub>, CuO și BaCO<sub>3</sub>.

### YBCO thin films characterization

The quality of a pyrolysed film is first indicated by its surface. The surface of the YBCO films after pyrolysis has to be smooth, without cracks or defects. According to the thermal analyses, the precursor powder decomposition is completed after  $400^\circ\text{C}$ . Thus, the pyrolysis temperature was selected in the temperature range  $400^\circ\text{C} - 500^\circ\text{C}$ . The best results were obtained for the pyrolysis performed at  $500^\circ\text{C}$  in humid oxygen atmosphere. The pyrolysed YBCO film surface was investigated by optic microscopy. In figure 3 is presented the microphotography of the YBCO film surface pyrolysed at  $500^\circ\text{C}$  in humid oxygen atmosphere. As it can be seen, the pyrolysed film surface is crack-free, smooth and presents only a “comet – type” spinning defect.

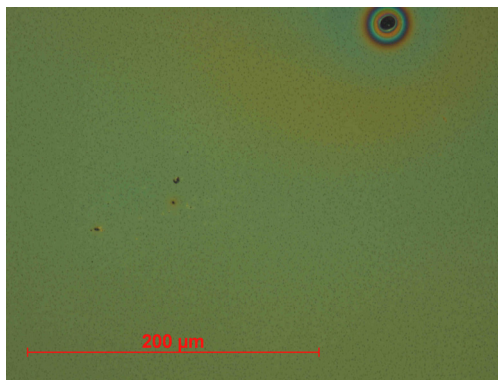


**Figure 3.** Microscopic image of the YBCO film pyrolysed at  $500^\circ\text{C}$  in humid oxygen atmosphere

The final YBCO films were structurally, morphologically and electrically investigated by X-ray diffraction, atomic force microscopy and by the four points method, respectively.

The structural investigation (presented in figure 4) indicates that the film has a high degree of (00l) orientation. The X-ray pattern of the crystallized YBCO film reveals only the presence of (00l)YBCO peaks and the peaks corresponding to the  $\text{SrTiO}_3$  (STO) single crystalline substrate. No other orientations of YBCO or other phases are detected. The peaks intensities reveal a good crystallization of the YBCO phase.

The three-dimensional characteristics of the particles were assessed by atomic force microscopy, AFM (figure 5). These investigations reveal a continuous surface with a small degree of porosity. Furthermore, the grains with the  $a/b$ -axis oriented perpendicular to the substrate are observed on the surface. These grains are not detected by the X-ray diffraction due to

the detection limit of the X-ray diffractometer (about 5%). From the AFM investigations the root-mean-square (rms) roughness and the peak-to-valley distance were calculated. It was found that rms roughness has the value of 36.5 nm and the peak-to-valley distance has the value of 472.8 nm, indicating a strong crystallization of the particles located on the film surface.

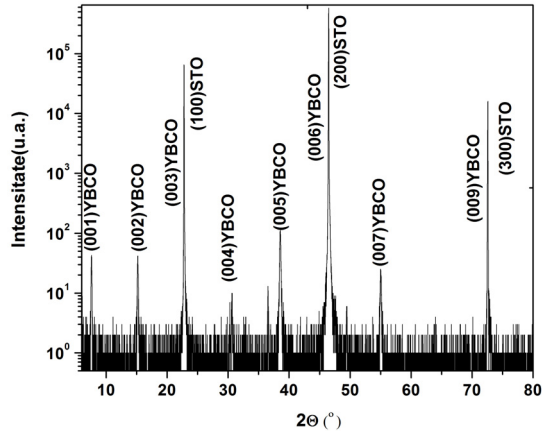


**Figure 4.** X-ray pattern for the YBCO film

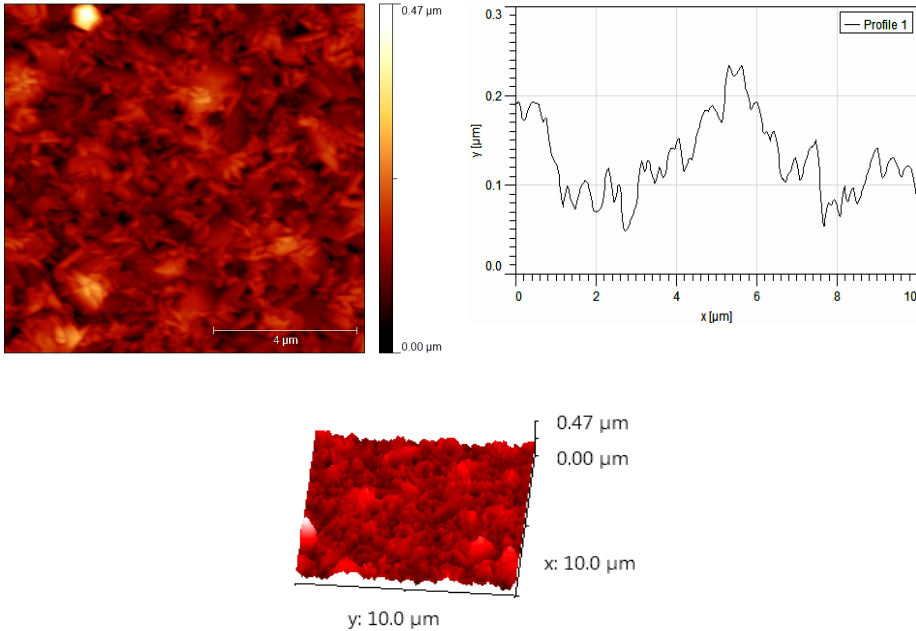


**Figure 5.** Two dimensional, 3D AFM images and the profile of an analysed line for the YBCO films

The electrical characterization of the YBCO films was performed using the four points method. In figure 5 is presented the temperature dependence of the electrical resistance of the YBCO thin film. The transport measurements show a transition temperature to the superconductive state of the YBCO thin film of 88.7K, with a  $\Delta T_c \sim 3\text{K}$ .

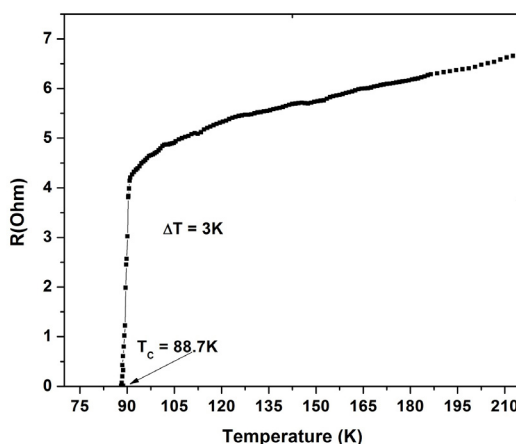


**Figure 6.** Temperature dependence of the electrical resistance of the YBCO film

## CONCLUSIONS

A fluorine-free water-based solution was prepared starting from metal acetates dissolved in water and propionic acid. In order to optimize the low temperature thermal treatment, the precursor powder was subjected to thermal analyses. It was found that above  $400^\circ\text{C}$  the organic part of the precursor powder is completely decomposed to oxides. The precursor solution was deposited by spin coating on (100)STO single crystalline substrates and subjected to a single-step thermal treatment. The as-obtained YBCO films were structurally, morphologically and electrically characterized. The structural investigations show that the films are highly (00l) oriented. No other phases or other orientations were detected. The AFM measurements reveal a rms roughness of 36.5 nm and a peak-to-valley distance of 472.8 nm. The AFM images present characteristic cross-needles which represent unwanted a-axis crystallites growth. The needles grow parallel to the edge of the substrate.

The critical temperature is 88.7K with a  $\Delta T \sim 3\text{K}$ , indicating that the YBCO films have good superconducting properties.

All the investigations have proved that it is possible to obtain YBCO films with good superconducting properties from a fluorine-free water based solutions in a single step thermal treatment.

## EXPERIMENTAL SECTION

### 1. Precursor solution and precursor powder synthesis

The precursor solution was prepared starting from yttrium acetate –  $\text{Y}(\text{CH}_3\text{COO})_3 \cdot 4\text{H}_2\text{O}$  (Alfa Aesar), barium acetate –  $\text{Ba}(\text{CH}_2\text{COO})_2 \cdot \text{H}_2\text{O}$  (Alfa Aesar) and copper acetate –  $\text{Cu}(\text{CH}_3\text{COO})_2 \cdot \text{H}_2\text{O}$  (Alfa Aesar). These acetates were individually dissolved in deionized water and an excess of propionic acid. Ammonium hydroxide was added to the Ba and Cu solutions until they become clear. The as-obtained solutions were mixed in an ultrasound bath for about 10 minutes and then concentrated by vacuum distillation under severe conditions. The stoichiometric ratio of the metal ions in the final precursor solution is Y:Ba:Cu = 1:2:3. The concentration of the metal ions in the final precursor solution is 1.5M.

### 2. Precursor powder characterization

In order to obtain the precursor powder, the as-prepared precursor solution was dried on a hot plate at 60°C in air. The as-obtained precursor powder was subjected to thermal analyses (DTA – TG) using a Q – derivatograph. The thermal analyses were performed both in dry, and humid oxygen atmosphere from room temperature up to 500°C with the following heating rates: from room temperature to 200°C with 5°C/min, from 200°C to 300°C with 3°C/min and from 300°C to 500°C the samples are heated with 2°C/min, to simulate the pyrolysis thermal treatment of the YBCO thin films.

### 3. Film deposition, thermal treatment and characterization

The precursor solution was spin coated on  $\text{SrTiO}_3$  (STO) single crystalline substrates with a spinning rate of 6000 rpm for about 120 seconds. The as-deposited precursor film was subjected to a single-step thermal treatment, as shown in figure 6. The thermal treatment takes place in a tube furnace under controlled atmosphere.

The single-step thermally treated YBCO thin films are structurally, morphologically and electrically characterized. The structural investigations were made by X-ray diffraction using an X Brucker AXS Discover 8 diffractometer ( $\text{Cu K}\alpha = 0.1541 \text{ nm}$ ). The X-ray diffractometer has a detection limit of 5% (in order for a crystalline phase to be detected it has to be in amount of more than 5%).

Atomic force microscopy was used to characterize the films morphology. The morphological investigations were made using a Veeco Dimension 3100 atomic force microscop. The electrical properties of the YBCO films were determined by Rvs.T measurements by using the four-probe technique.



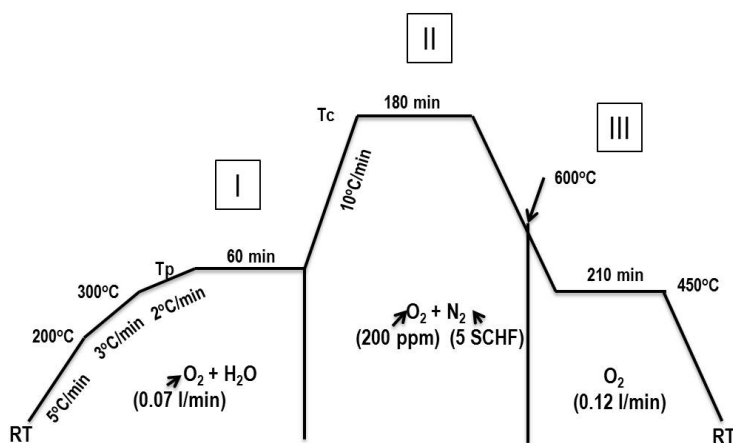


**Figure 7.** The thermal treatment diagram for YBCO films  
I – pyrolysis ( $T_p = 500^\circ\text{C}$ ); II – crystallization ( $T_c = 850^\circ\text{C}$ ); III - oxygenation

## ACKNOWLEDGMENTS

This paper was supported by the project “Doctoral studies in engineering sciences for developing the knowledge based society-SIDOC” contract no. POSDRU/88/1.5/S/60078, project co-funded from European Social Fund through Sectorial Operational Program Human Resources 2007-2013 and partially by CNCIS – UEFISCU, project number PN II – IDEI cod 106/2010.

## REFERENCES

1. L. Ciontea, T. Petrișor, A. Giurgiu, *Applied Superconductivity, World Congress on Superconductivity Proceedings of the 3<sup>rd</sup> International Conference and Exhibition, 1993*, 1, 853 – 857.
2. A. Armenio, A. Augieri, L. Ciontea, G. Contini, I. Davoli, V. Galluzzi, A. Mancini, A. Rufoloni, T. Petrișor, A. Vannozzi, G. Celentano, *Superconductor Science and Technology*, **2008**, 21, 7.
3. W. Cui, J.L. Tanner, T.W. Button, J.S. Abell, *Journal of Physics: Conference Series*, **2008**, doi: 10.1088/1742-6596/97/1/012257.
4. X. Obradors, T. Puig, A. Pomar, F. Sandiumenge, N. Mestres, M. Coll, A. Cavallaro, N. Romà, J. Gazquez, O. Castaño, J. Gutierrez, A. Palau, K. Zalamova, S. Morlens, A. Hasini, M. Gibert, S. Ricart, J.M. Moretó, S. Piñol, D. Isfort, J. Bock, *Superconductor Science and Technology*, **2006**, 19, S13 – S26.

5. T. Araki, I. Hirabayashi, *Superconductor Science and Technology*, **2003**, 16, R71 – R97.
6. I. Yamaguchi, M. Sohma, K. Tsukada, W. Kondo, K. Kamiya, S. Mizuta, T. Kumagai, *IEEE Transactions on Applied Superconductivity*, **2005**, 15, 2927 – 2930.
7. Y. Zhang, X. Yao, J. Lian, L. Wang, A. Li, H. K. Liu, H. Yao, Z. Han, L. Li, Y. Xu, D. Shi, *Physica C*, **2006**, 436, 62 – 67.
8. P. Vermeir, I. Cardinael, M. Backer, J. Schanbroeck, E. Schacht, S. Hoste, I. Van Driessche, *Superconductor Science and Technology*, **2009**, 22, 075009.
9. M. Nasui, R.B. Mos, T. Petrisor Jr., M.S. Gabor, R.A. Varga, L. Ciontea, T. Petrisor, *Journal of Analytical and Applied Pyrolysis*, **2011**, doi:10.1016/j.jaap. 2011.08.005